PHYSICAL REVIEW C VOLUME 42, NUMBER 2 AUGUST 1990

Effects of nuclear deformation on $^{151,153}Eu(p,n)^{151,153}Gd$ reactions

R. G. Lanier, H. I. West, Jr., and M. G. Mustafa
Nuclear Chemistry Division, Lawrence Livermore National Laboratory, Livermore, California 94550

J. Frehaut, A. Adam, and C. A. Philis
Service de Physique et Techniques Nucleaires, Centre d'Etudes Bruyeres-le-Chatel, Boîte Postale No. 12, 91680 Bruyeres-le-Chatel, France

(Received 9 April 1990)

Total cross sections for the $^{151,153}Eu(p,n)^{151,153}Gd$ reactions have been measured between 5 and 12 MeV. We observe a significant ($\leq 35\%$) enhancement of the cross sections for ^{153}Eu relative to ^{151}Eu and find that the enhancement below ~ 10 MeV is due largely to the shape difference between ^{151}Eu ($\beta_2 = 0.13$) and ^{153}Eu ($\beta_2 = 0.28$).

In a recent experiment, we used targets of natural europium to accurately measure the $^{151,153}Eu(p,n)^{151,153}Gd$ excitation functions between 5 and 12 MeV. We find that the cross sections for ^{153}Eu, $\sigma(153)$, in the rising portion of the excitation function are enhanced relative to those for ^{151}Eu, $\sigma(151)$. This observation is particularly interesting because it is consistent with nuclear structure work in the europium, $N = 89$, region. These studies document significant changes in nuclear properties due to a drastic change in the equilibrium ground-state shape.[1] In this Rapid Communication we present evidence that the behavior of our measured cross sections is due to the shape difference[1] between ^{151}Eu ($\beta_2 = 0.13$) and ^{153}Eu ($\beta_2 = 0.28$).

An observation similar to ours has been noted in neutron total cross-section [$\sigma_n(T)$] measurements for the even-even Nd and Sm isotopes.[2-4] To our knowledge, however, ours is the first measurement which shows an "enhancement" with charged particles and which isolates the effect for a specific reaction channel. We find that our measured enhancements are nearly an order of magnitude larger than those from the $\sigma_n(T)$ measurements. We discuss some features of this comparison later in the text.

Our experiments were carried out at the tandem Van de Graaff facility at Centre d'Etudes, Bruyeres-le-Chatel, France (CEB). We used beams of protons in the energy range between 6 and 12 MeV to irradiate single- and multiple-foil stacks of specially fabricated targets of natural Eu_2O_3. The targets were made by thoroughly mixing chemically pure Eu_2O_3 with a polyimide resin,[5] thinly spreading the mixture over a smooth surface, and then curing the material at ~ 260 °C to form sheets. From these sheets, target foils 25.4 mm in diameter were cut that had areal densities of ~ 15 mg/cm^2. Approximately one third of the density was due to elemental Eu. The foils were intercompared for homogeneity and areal density of Eu by x-ray fluorescent spectroscopy. Selected foils were assayed by gravimetric methods to determine the weight percent of Eu metal. This provided an absolute calibration for the relative areal density measurements made by x-ray fluorescence. Only foils uniform to better than 2% were used for the irradiations. The areal densities were determined to an uncertainty of $\leq \pm 1\%$.

During an irradiation, the beam incident on a target was swept in a square 8×8 mm to minimize heat loading and to ensure that any small nonuniformities in the foil would cause no substantial error in the cross-section measurement. The ^{151}Gd and ^{153}Gd γ-ray activities from the foils were measured on large-volume germanium detectors at the radiation counting facility of CEB. Measured decay rates were converted to the number of Gd atoms produced during the irradiation using the decay scheme information[6-9] in Table I, and by using the isotopic abundance[10] values for natural europium of 47.8% for ^{151}Eu and 52.2% for ^{153}Eu.

Since the target foils had a total thickness of ~ 15 mg/cm^2, the beam suffered significant energy degradation during its passage through a single foil. We calculated the energy losses through individual foils and through foil stacks which were composed of as many as three Eu foils interleaved with thin Al-degrader foils. The energy loss through a typical foil was 0.4–0.6 MeV for 10-MeV protons. Depending on the number of foils in a stack, the losses could accumulate to several MeV at the lowest beam energies. To check the accuracy of our energy-loss

TABLE I. Decay scheme data for $^{151,153}Gd$.

	^{151}Gd ($t_{1/2} = 125.6$ d)[a]		
E (keV)	153.6	174.7	243.2
I_γ (%)	6.20[b]	2.98[c]	5.58[c]
	^{153}Gd ($t_{1/2} = 237.9$ d)[a]		
E (keV)	97.43	103.18	
I_γ (%)	27.60[d]	20.45[c]	

[a]The half-lives are recent measurements due to Nethaway (Ref. 6).
[b]The I_γ for the 153.6-keV γ of ^{151}Gd is the average of 6.1 (5%) of Ref. 7 and 6.3 (4%) of Ref. 8.
[c]The other γ-ray intensities were adjusted slightly from those in the literature to fit the relative intensities measured at CEB.
[d]The I_γ for the 97.43-keV γ ray is from Ref. 9.

calculations, we measured the energy loss experienced by protons through single foils and through foil stacks. These measurements were conducted at several incident particle energies in the range 3–12 MeV. The calculated energy losses agree with the measured values to better than 3%.

The results of our measurements are shown in Fig. 1 as a plot of $[\sigma(153)-\sigma(151)]/\sigma(151)$ vs E, where E is the effective energy of the protons in the foils. The feature we wish to emphasize in Fig. 1 is the clear enhancement of the ^{153}Eu cross sections relative to those measured for ^{151}Eu. The scatter of the data reflects uncertainties associated with individual foil uniformity, beam energy, beam-current integration, and counting statistics. Because we used foils which were homogeneous-isotopic mixtures of ^{151}Eu and ^{153}Eu, any uncertainty in proton energy would not alter the data comparison. However, the positions of the enhancement ratios on the energy scale are affected by energy errors, but these errors are ≤ 100 keV and are not significant in Fig. 1. In addition (see Table I), for the ^{151}Gd data we have an uncertainty in I_γ of $\pm 3\%$ and for ^{153}Gd an uncertainty of $\pm 5\%$. In Fig. 1, the shaded area noted represents the upper and lower bounds on our data that could result from the I_γ uncertainties. The other uncertainties discussed previously affect the data comparison in only a minor way.

A simple comparison[11] of ^{151}Eu and ^{153}Eu shows that these nuclei are similar; they are adjacent odd-A nuclei with identical ground-state spins and parities ($\frac{5}{2}^+$). Thus, our observed enhancements cannot be due to entrance-channel angular momentum differences. Also, it is highly unlikely that the enhancements are due to differences in the energetics governing the reaction processes. The Eu-Gd mass differences are virtually identical[12] ($\Delta 151 = -465 \pm 5$ keV, $\Delta 153 = -484 \pm 5$ keV), therefore, the reaction thresholds are nearly equal. Thus, with these conditions and using simple optical- and statistical-model arguments, we would expect only small differences in the cross sections if both target nuclei were spherical. This conclusion is confirmed by a statistical-model calculation[13] with spherical optical model potentials.[14] The result is shown in Fig. 1 (curve SPH). Note that the conventional definition of nuclear radius $R = R_0 A^{1/3}$ gives only $\sim 0.4\%$ radius difference between ^{151}Eu and ^{153}Eu. However, if these calculations are performed with an $\sim 3\%$ larger radius for ^{153}Eu, we can reproduce the enhancements observed. This supports the conclusion that our data can be accounted for, if we properly include entrance-channel nuclear-shape differences in our calculations.

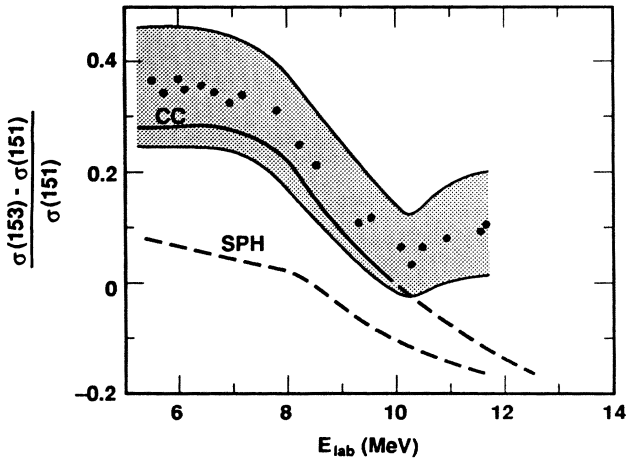

FIG. 1. The (p,n) cross-section differences for ^{153}Eu and ^{151}Eu, divided by the ^{151}Eu(p,n) cross section. The upper and lower bounds of the shaded area indicate the maximum range that could occur in the interpretation of the data due to uncertainties of $\pm 3\%$ in I_γ's for ^{151}Gd and $\pm 5\%$ for ^{153}Gd. The lines labeled CC and SPH refer to our theoretical calculations for coupled-channel and spherical-optical models, respectively.

To consider such an effect more quantitatively, we estimated the theoretical (p,n) cross sections by combining results from a spherical-statistical-model (SPH) calculation[13] with those obtained from the coupled-channel (CC) code JUPITOR,[15] which explicitly accounts for deformation effects. We first used the code to calculate the reaction cross section $\sigma(R)$ for the ^{151,153}Eu$+p$ reactions between 5 and 12 MeV using collective-model parameters previously published.[1] For ^{151}Eu, we treated the nucleus as an odd-A vibrator and coupled the 0-, 196-, 308-, and 506-keV states to a single one-phonon excitation with $\beta_2 = 0.13$ in a nonadiabatic mode (NACC). These states are the most strongly excited states in (p,p') studies[1] and are believed to have the following[11] spin parities, respectively: $\frac{5}{2}^+$, $\frac{3}{2}^+$, $\frac{5}{2}^+$, and $\frac{7}{2}^+$. We treated ^{153}Eu in an adiabatic approximation mode (ACC) which effectively couples all the rotational members of the ground band. The coupling schemes noted above are justified by nuclear structure arguments along with the data presented in Ref. 1. For the nuclear potential, we used the Becchetti-Greenless (BG) spherical optical-model potential given in Ref. 14, but adjusted the surface term W_D downward by 20% to account for our explicit treatment of the inelastic channels. For these calculations, we used complex coupling throughout, and for ^{153}Eu we used $\beta_2 = 0.28$ and included the effect of $\beta_4 = 0.06$.

Instead of a coupled-channel Hauser-Feshbach statistical-model calculation, we made the following approximate calculation to determine the (p,n) cross sections. We ran the statistical model code STAPRE (Ref. 13) to calculate the reaction and (p,n) cross sections with the nonadjusted BG spherical[14] potential. We can assume to good approximation that at low energies the (p,n) to reaction cross-section ratios are equal for both the spherical-statistical model and a more realistic calculation for the deformed nuclei using the CC formalism. Thus, we can write $\sigma(p,n)_{CC} = \sigma(R)_{CC}[\sigma(p,n)_{SPH}/\sigma(R)_{SPH}]$. The procedure carries with it the implicit assumption that the spin distribution for $\sigma(R)_{CC}$ is the same for $\sigma(R)_{SPH}$. The assumption is expected to be valid at lower energies where the inelastic cross sections are small. At higher energies, the effects of the inelastic channels on the spin distribution become progressively more important and our procedure becomes less valid. Also, at low energies, the only competing channel comes from the (p,γ) process. However, for $E_p > 7.5$ MeV the $(p,2n)$ channels open; thus, for $E_p \geq 10$ MeV, where these cross sections become appreciable, we can expect additional difficulties from this

procedure.

In Fig. 1, we show the results of our calculated enhancements from a spherical-optical-model calculation (SPH) and from the coupled-channel calculations (CC) with the deformed potentials. The enhancements calculated from the spherical-statistical model are due completely to the mass and isospin dependence in the optical potential[14] and in the level-density prescription.[16] These calculations miss the data generally by a factor of three and are therefore quite inadequate to account for our observations. By using the coupled-channel formalism with deformed potentials, however, we significantly improve the agreement for $E_p < 10$ MeV. We remark here also that our CC calculated (p,n) excitation functions agree very well with the experimental data at low energies but begin to depart noticeably from the measurements at $E_p \sim 9$ MeV.

The general disagreement between our calculations and experiment beyond 9–10 MeV is due primarily to an improper characterization of the statistical-model parameters associated with the $(p,2n)$ competition. We have used only global optical potentials and the level densities from a Gilbert-Cameron prescription[16] with parameters from Rose and Cook.[17] Further refinements in the calculations will require a better characterization of these model features in the $A \sim 150$ region. Thus, with the present form of the calculations and given the approximation made, making parameter adjustments to better fit the data at higher energies is unwarranted. Clearly, it would be most desirable to obtain the (p,n) cross sections for both nuclei from a statistical model that uses the coupled-channel formalism. At low energies, where we have good agreement with our calculations, there is only one minor competing channel $[(p,\gamma)]$ and the effect of the inelastic channels is relatively small. However, as the projectile energy increases, this coupling becomes progressively more important and would be expected to be a non-negligible feature in any realistic calculations for higher energy (p,xn) processes.

We mentioned in the introduction that the measured deformation-dependent enhancement for $\sigma(p,n)$ is much larger than the same enhancement for the total neutron cross section $[\sigma_n(T)]$. Some of the difference between these two enhancements can be attributed to the large neutron shaped elastic cross section that is included in $\sigma_n(T)$. In order to understand this comparison more thoroughly and also because of the fact that $\sigma(p,n)$ is nearly equal to the absorption cross section $[\sigma(R)]$ over most of the energy range covered by our measurements, we have investigated[18] the deformation dependence of $\sigma(R)$ for proton and neutron reactions with ^{151}Eu and ^{153}Eu. We have used the BG (Ref. 14) potential and a recently evaluated potential for ^{151,153}Eu by Macklin and Young.[19] We show that the deformation-dependent enhancement in $\sigma(R)$, in general, is much larger for protons than for neutrons. Although the cross-section magnitude produced by each potential is different, a significantly larger enhancement for protons over neutrons is a consistent feature of these calculations. We also mention that the larger cross section enhancement of protons over neutrons still prevails even if the contributions of the inelastic channels are added to $\sigma(R)$.

We believe that our data provide an excellent and unique opportunity to test reaction-model calculations in spherical and deformed nuclei. In addition to the data described here, we have also measured $(d,2n)$ excitation functions for the same target nuclei. The data show enhancements for deuterons similar to those for protons. However, the analyses are still preliminary and the results will be reported later. Additional data for $E > 11$ MeV for both protons and deuterons are also being acquired and will be used to identify any shape effects at higher energies using more realistic coupled-channel Hauser-Feshbach calculations.

Two of us (R.G.L. and H.I.W.) wish to thank the staff at CEB for their help and hospitality throughout the course of the work at CEB. We are also grateful to Ruth Nuckolls for her work with the target density measurements. This work was performed under the auspices of the U.S. Department of Energy by Lawrence Livermore National Laboratory, Contract No. W-7405-ENG-48 and under the auspices of the Commissariat a l'Energie Atomique of France.

[1]R. G. Lanier, L. G. Mann, G. L. Struble, I. D. Proctor, and D. W. Heikkinen, Phys. Rev. C **18**, 1609 (1978), and references therein.

[2]R. E. Shamu, E. M. Bernstein, J. J. Ramirez, and Ch. Lagrange, Phys. Rev. C **22**, 1857 (1980).

[3]C. Y. Wong, T. Tamura, H. Marshak, and A. Langsford, Part. Nucl. **4**, 163 (1972).

[4]R. E. Shamu, E. M. Bernstein, D. Blondin, J. J. Ramirez, and G. Rochau, Phys. Lett. **45B**, 241 (1973).

[5]The equivalent of "Kapton," which is a plastic product marketed in sheets by the E. I. Du Pont de Nemours & Co., Inc., Wilmington, DE, 1989.

[6]D. R. Nethaway (private communication).

[7]K. E. Gregorich, J. J. Moody, and G. T. Seaborg, Radiochem. Acta. **35**, 1 (1984).

[8]E. Voth, W. D. Schmidt-Ott, and H. Behrens, Z. Phys. A **313**, 167 (1983).

[9]E. Browne and R. B. Firestone, *Table of Radioactive Isotopes,* edited by V. S. Shirley (Wiley, New York, 1986).

[10]*Chart of the Nuclides,* General Electric Nuclear Energy Division, San Jose, CA 95125. Revised April 1972.

[11]E. Browne, J. M. Dairiki, and R. E. Doebler, *Table of Isotopes,* edited by C. M. Lederer and V. S. Shirely (Wiley, New York, 1978).

[12]A. H. Wapstra and G. Audi, Nucl. Phys. **A432**, 1 (1985).

[13]D. G. Gardner, Nuclear Chemistry Division, Lawrence Livermore National Laboratory, Livermore, CA 94550, modified version of the Code STAPRE, originally written by B. Strohmaier and M. Uhl, Institut fur Radiumforschung und Kernphysik (Vienna) Report No. IRK 76/01 with Addenda, 1976 (unpublished).

[14]C. M. Perey and F. G. Perey, At. Data Nucl. Data Tables **17**,

1 (1976).

[15]T. Tamua, Rev. Mod. Phys. **37**, 679 (1963); and The JUPITOR Code Instructions, T. Tamura, Oak Ridge National Laboratory Report No. ORNL-4152 (unpublished).

[16]A. Gilbert and A. G. W. Cameron, Can. J. Phys. **43**, 1446 (1965).

[17]E. K. Rose and R. L. Cook, Australian Atomic Energy Commission Report No. AAEC/E419, 1977 (unpublished).

[18]M. G. Mustafa, Nuclear Chemistry Division Annual Report, Lawrence Livermore National Laboratory Report No. UCAR 10062-89, 1989 (unpublished), p. 63.

[19]R. L. Macklin and P. G. Young, Nucl. Sci. Phys. Eng. **95**, 189 (1987); P. G. Young (private communication).

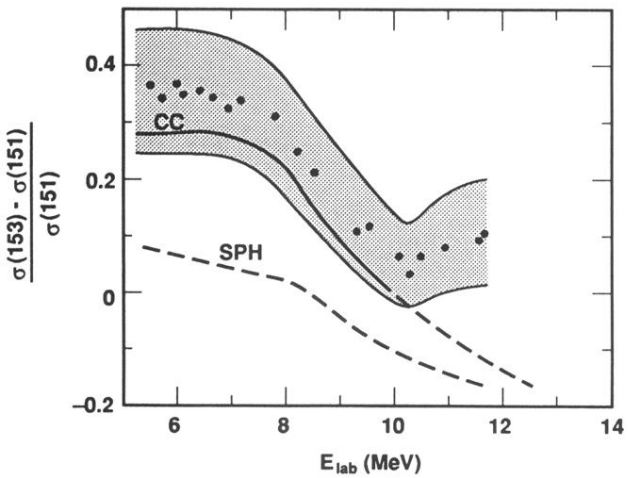

FIG. 1. The (p,n) cross-section differences for ^{153}Eu and ^{151}Eu, divided by the ^{151}Eu(p,n) cross section. The upper and lower bounds of the shaded area indicate the maximum range that could occur in the interpretation of the data due to uncertainties of $\pm 3\%$ in I_γ's for ^{151}Gd and $\pm 5\%$ for ^{153}Gd. The lines labeled CC and SPH refer to our theoretical calculations for coupled-channel and spherical-optical models, respectively.